Available online at www.sciencedirect.com

SciVerse ScienceDirect

Procedia Engineering 59 (2013) 183 – 192

Procedia Engineering

www.elsevier.com/locate/procedia

3rd International Conference on Tissue Engineering, ICTE2013

3D hybrid bioprinting of macrovascular structures

Can Kucukgul[a], Burce Ozler[a], H. Ezgi Karakas[b], Devrim Gozuacik[b], Bahattin Koc[a]*

[a]*Sabanci University, Manufacturing and Industrial Engineering, Faculty of Engineering and Naturel Sciences, Istanbul,34956, Turkey*
[b]*Sabanci University, Bioengineering, Faculty of Engineering and Naturel Sciences, Istanbul,34956, Turkey*

Abstract

Thousands of people die each year due the cardiovascular health problems. The most common treatments for cardiovascular health diseases are autografts and blood vessel transplantations which has limitations due to lack of donors and the patient's conditions. Although there are several scaffold based studies about vascular tissue engineering, scaffold-based vascular grafts have some side effects including chronic inflammation, thrombosis and rejection after *in-vivo* implantation. Additionally, there are some problems with cell to cell interaction, the assembly and alignment of ECM components and the host response to scaffolds. Therefore, vascular tissue engineering studies tend towards scaffold- free techniques. In this paper, novel computer aided algorithms and methods are developed for 3D printing of scaffold-free macrovascular structures. An example aorta model is generated using imaging and segmentation software. The developed algorithms are implemented using Rhinoscript. In order to support printed cell aggregates, support structures with 'Cake' and 'Zigzag' patterns are developed and 3D printed.

Selection and peer-review under responsibility of the Centre for Rapid and Sustainable Product Development, Polytechnic Institute of Leiria, Centro Empresarial da Marinha Grande.

Keywords: scaffold free vascular tissue engineering, computer aided biomodeling, 3D bioprinting , hybrid cell-biomaterial printing.

* Corresponding author. Tel.: +90-216-4839557; fax: +90-216-483-9550.
E-mail address: bahattıinkoc@sabanciuniv.edu

Selection and peer-review under responsibility of the Centre for Rapid and Sustainable Product Development, Polytechnic Institute of Leiria, Centro Empresarial da Marinha Grande
doi:10.1016/j.proeng.2013.05.109

1. Introduction

Cardiovascular disease is the leading cause of deaths worldwide and annually thousands of patients die because of this type of diseases. Autografts and blood vessel transplantation are the most common treatments in cardiovascular diseases. Using autografts may not be possible because the donor site may not have enough autografts or the patient's health condition may not allow harvesting one. Recently, tissue engineering and regenerative medicine aim to provide alternative treatments and fast recovery for the patients suffering from cardiovascular diseases [1].

Traditionally, tissue engineering strategies are based on the cell seeding into synthetic, biological or composite scaffolds providing a suitable environment for cell attachment, proliferation and differentiation. Although 3D scaffolds are designed to act as an artificial extracellular matrix (ECM) until the cells form their own ECM, it is challenging to fabricate a controlled porous structure with the desired internal architecture repetitively. In addition, the functional vascularization of the 3D scaffold is compulsory for nutrition and oxygen supply. In order to provide nutrition and oxygen to the cells, different approaches based on endothelial cells or scaffolds are developed [2].

To enable the direct anastomosis of the scaffold to the host vasculature *in vivo*, self-assembly approaches are used. In this approach, a bioprinted macrovascular network is matured in a perfusion reactor to achieve the required mechanical properties. Microvascular units in the form of cylindrical or spherical multicellular aggregates are produced by the parenchymal and endothelial cells, placed in the macrovascular network and perfused to promote self-assembly and the connection to the existing network [3].

Despite several studies related with the vascular tissue engineering, it is still not achieved to construct an entirely biomimetic blood vessel due to the poor mechanical properties of the materials. Therefore, first applications of scaffold-based vascular grafts are tried under low pressure. The degradation of the materials and the cell-material interaction could cause unforeseen side effects including chronic inflammation, thrombosis and rejection after *in-vivo* implantation. Especially, weakness of cell to cell interaction and the assembly and alignment of ECM are critical in vascular tissue-engineering. Considering all these reasons, vascular tissue engineering studies tend towards scaffold- free techniques [4].

In the literature, there has been few research working on building small-diameter, multi-layered, tubular vascular and nerve grafts [5]. Multicellular spherical and cylindrical aggregates have been fabricated with 3D printing methods. Flexibility in tube diameter and wall thickness is obtained and most significantly branched macrovascular structures are constructed with this method [5]. In another study, human embryonic stem cell spheroid aggregates are formed with a valve-based cell printer and they have controllable and repeatable sizes. This work shows that the printed cells are mostly viable and have the potential to differentiate into any of the three germ layers (pluripotency) [6]. However, the preparation of large amounts of spherical aggregates is time-consuming and the fusion process of the spheroids takes 5-7 days. Alternatively, cylindrical cell aggregates (bioink) allow producing more controlled structure in a short time. Additionally, cylindrical bioinks are fused within 2-4 days [4]. However, it is challenging to 3D print tissue constructs with cylindrical bioinks.

The main objective of this paper is to develop a novel computer aided algorithms to model and 3D bioprint of multi-cellular cylindrical aggregates and their support structures with biomaterials (hydrogels) to enable scaffold-free tissue engineering of blood vessels. In addition, 3D bioprinting tool path planning and parameters are optimized in this paper. The computer aided algorithms are developed to enable a fully biological scaffold-free tissue engineering methodology.

2. Planning for 3D hybrid bioprinting

2.1. 3D Imaging

In order to 3D bioprint a blood vessel, the geometry of the blood vessel needs to be captured and used in computer aided modelling. To demonstrate the methodology, a human aorta vessel is chosen. Medical images of the aorta could be obtained by Magnetic Resonance Imaging (MRI) and Computer Tomography (CT). The MRI or CT images need to be segmented and converted to 3D computer models. Mimics software is used for segmentation

and region growing. A sample MRI data provided with Mimics software is used for biomodeling. A part of abdominal aorta model from MRI slices are used.

In Mimics, a segment of the aorta is first masked using masking tool. Then, the region growing is implemented to connect the slices of aorta to convert into 3D mesh model. To obtain a single macrovascular structure, small vascular links between aorta and other tissues structures are determined at each slice and they are separated. Figure 1. (a-c) shows the process for obtaining the macrovascular geometry of the aorta. Then, the region growing is implemented to connect the slices of aorta to convert into 3D mesh model. The mesh file is then converted to an STL (StereoLithography) file (Fig. 1 (d-f), which will be used for computer-aided modeling methodology described at the next sections.

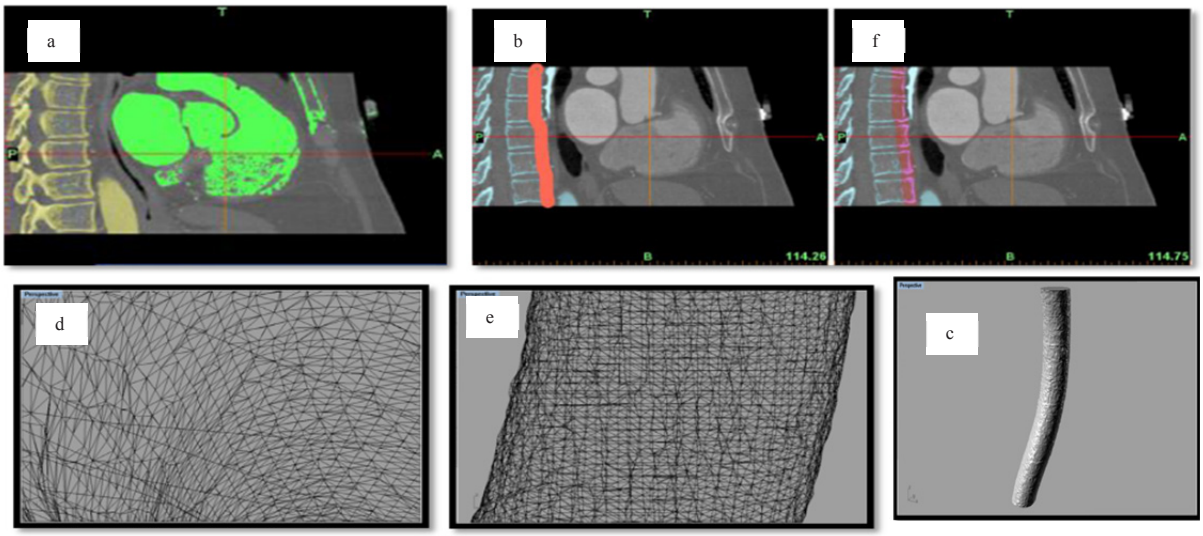

Fig. 1. (a-c) Segmentation of an aorta from a spine process based on region growing; (d-f) STL file of the aorta, mesh structure.

2.2. Biomodeling of Aorta

After the mesh model of the aorta is obtained using Mimics software. The resultant STL model of the aorta model is not smooth and represented with meshes. To be able to develop path planning and optimization the STL model needs to be represented by freeform surface information. The aorta model with its support structure is represented by:

$$O = (F, R, M, C);\ F = \{ \{FF_a\}_{a=0,\ldots,A}, \{GF_b\}_{b=0,\ldots,B} \} \in E^3, R = \{ R_{a_1 a_2} \}\ a_1 = 0,\ldots,A; a_2 = 0,\ldots,A; a_1 \neq a_2$$

$$\mathbf{M} = \left\{ \{M_k, f^{(k)}(r,s,t)\}_{k=1,\ldots,n} \right\}\ \{M_k\} \in M^n\ \ C = \{C_b\}_{b=0,\ldots,B} \tag{1}$$

Where, O represents the aorta model's geometric and cell-biomaterial parametric and mathematical information and relationship. Since aorta and other biomedical objects are represented ın free-form shapes, each of the geometric features $\{FF_a\}_{a=0,\ldots,A}$, are represented with B-spline functions of parameters *u* and *v:*

$$FF_a(u,v) = \sum_{i=0}^{\alpha}\sum_{j=0}^{\beta} N_{i,p}(u)\, N_{j,q}(v)\, P_{i,j,a} \qquad (2)$$

The geometric constraint set, **R**, specify the relationships between the various form features of the object. The aorta model **O** now has $B + 1$ number of cell-biomaterial geometric features $\{GF_b\}$, $b = 0, ..., B$ and cell-biomaterial functions **M**. The material variation is constrained using function **C** with at least one geometric reference entity – a material governing feature. This form of representation is necessary because whenever a cell-biomaterial governing feature is changed, it is desired that the related material features should also change accordingly.

In order to convert the STL model of aorta to B-spline surfaces geometric features $\{FF_a\}_{a = 0, ..., A}$, the STL model is first sliced and contours are generated. Each contour is made out of polylines and are not smooth. The contour polylines are interpolated with B-spline curves as given as shown in Fig. 2(b). Then, each contours central location is determined to form the middle skeletal curve to fit a B-spline surface. Fig. 2(c) shows the smooth B-spline surface of the aorta model.

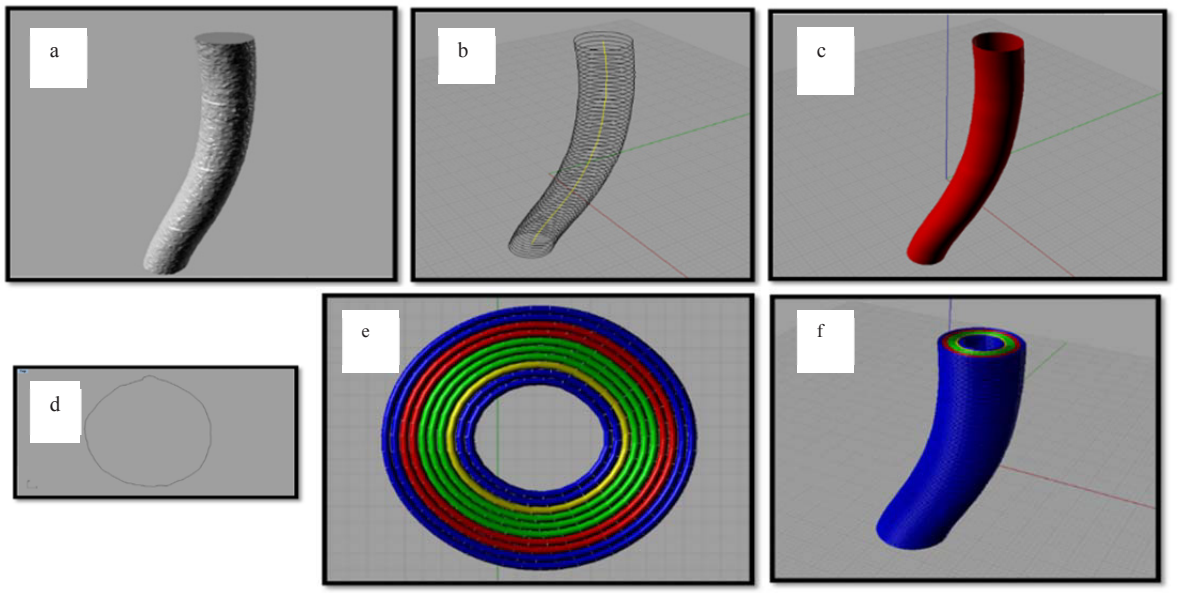

Fig. 2. (a) STL model of aorta vessel; (b) Construction of the skeleton curve from contour curves; (c) Final smoothed aorta vessel; (d) One contour curve, z-axis planar; (e) One layer of the aorta with whole cellular aggregates and support gels (outer-inner sections); (f) Final structure of an unsupported aorta.

As mentioned before, the generated CAD model will be used to 3D bioprint cell and support biomaterials layer by layer. Therefore, at each layer, the cell and biomaterial geometry $\{GF_b\}$, $b = 0, ..., B$ and composition **M** needs to be determined. To determine the layers, the B-spline surface of the aorta model is sliced again along the build direction. Fig. 2 (d) shows a contour after slicing.

Biomimicking the actual aorta model, different type of cell their geometry and composition is determined at each layer. At each layer surrounding support layer is also determined. Fig. 2(e) shows a single layer with cylindrical cell aggregates. Blue color is used to represent support biomaterial, red shows fibroblast, green is for smooth muscle cells and yellow is for endothelial cells. Figure 2(f) shows whole aorta model **O** with cell and support biomaterial structure is given.

2.3. Support structure generation and path planning

After each layer with cell composition is determined this cylindrical aggregates of the cell will be printed using a 3D bioprinter layer by layer. Therefore each cylindrical cell layer needs to be supported and path planning for cell-biomaterial topology needs to be determined. To develop support structures and path planning for 3D printing computational algorithms are developed. Two approaches are used for support generation. The first approach was to develop a support structure that basically support itself layer by layer. Starting from top layer, we offset each contour by a diameter of support material for inner and outer supports. When we moved to each layer, the previous cylinders (cell aggregates and support material) are supported by two cylinders at their bottom layer. This continues until the final bottom layer is reached. As shown in Fig. 3, the shape looks like a cake, therefore this method is called cake support. As shown in the figure, each layer is always supported and this provides better and stable cell aggregate printing since the cell aggregates may not be as strong as the biomaterial.

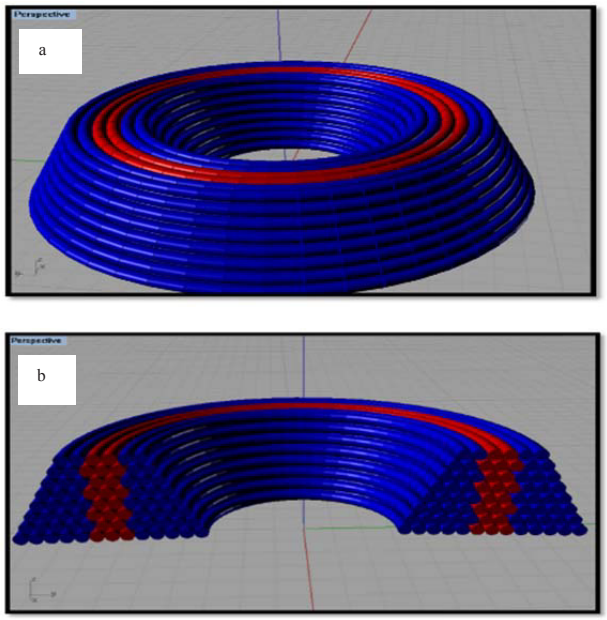

Fig. 3. (a-b) Cake model implementation, in whole shape and a cross-sectional half (red:cell aggregates, blue: support).

This type of support generation may be suitable for a hollow like tissues such as an aorta. However, this cannot be applied to any type of tissues or organs. Therefore, we also developed another approach and algorithms to generate support structure using traditional zig-zag pattern. First As shown in Fig. 4, at each layer 0-90 degree support structures (cylinders) are used to support previous layer. First, the bounding box of the aorta model is calculated. The bounding box is ten offset along the layer direction to generate support structures. After the offset bounding box is found, the support structure and aorta model is sliced. At each layer, the space between the bounding box and the aorta contour is filled with support material usıng a zig-zag pattern. A successive layers are shown in Fig. 4(a). Fig. 4(b-c) are showing the whole support structure totally enclosing the aorta model. As the structure illustrated, zigzag model has self supports both from the lower layers and from the inside curves.

After the support structure is determined, path planning is calculated for 3D bioprinting of cell aggregates and their support structure.

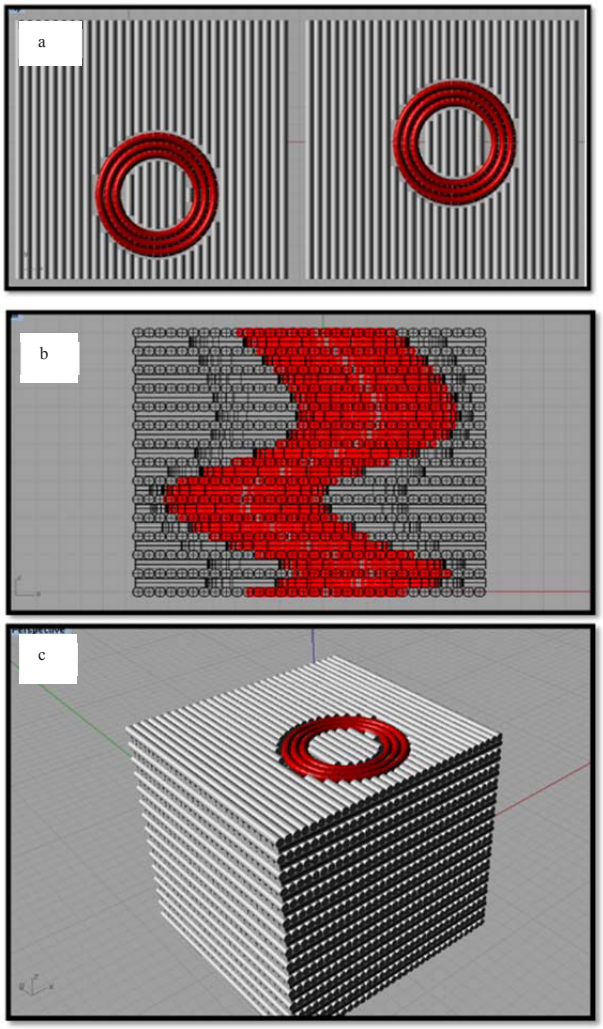

Fig. 4. (a) Top view of cell aggregates (red) and their support material. (b) Cross-sectional right view of the whole cell and support structure, (c) Perspective view of the whole cell and support structure enclosing the aorta model.

2.4. 3D Bioprinting

For hybrid 3D printing of cells with support biomaterials, Novogen MMX Bioprinter is used. The bioprinter can not only print hydrogel biomaterials but also cylindrical cell aggregates. The printer has two deposition head for support hydrogel and cells. The printer can be controlled with its own software for simple geometries. However, controlling scripts must be written for complex geometries. After determining the deposition paths, these are used to generate path planning scripts. Fig. 5 shows schematic illustration of the bioprinter (second cell head is being planned).

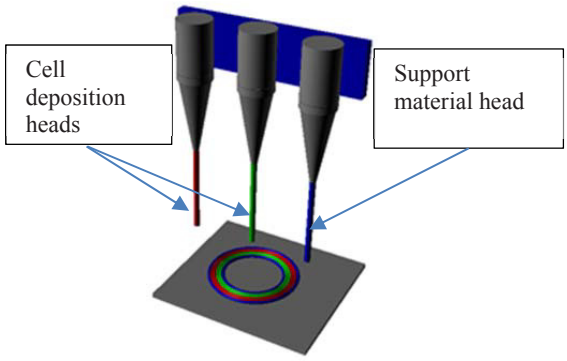

Fig. 5. Schematic illustration of bioprinter.

Fig. 6 shows the 3D bioprinter with various sample prints using Novogel hydrogel. As shown in the figure, the generated paths can be used for generating scripts which are then used to control the bioprinter. With the developed algorithms, the designed models can then be used to directly control the bioprinter which can print the cell aggregates and support hydrogels layer by layer for tissue formation.

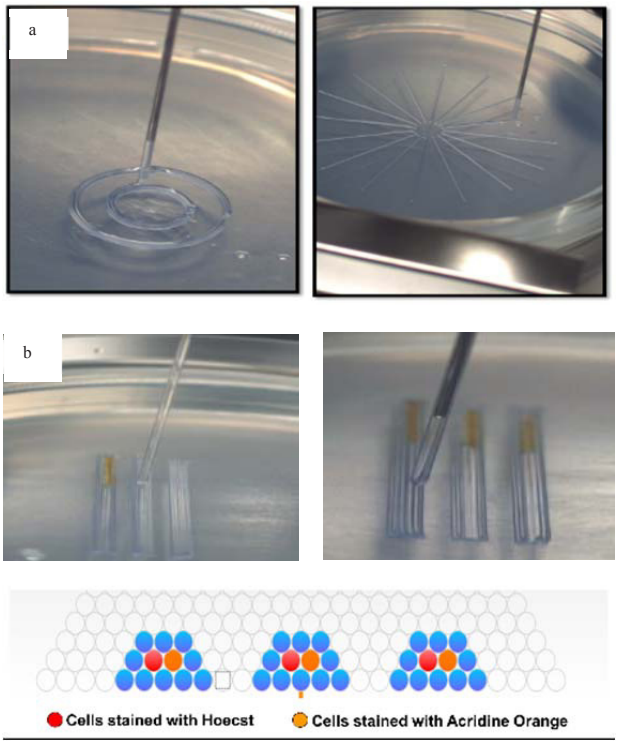

Fig. 6 (a) various printed hydrogels with Novogel hydrogel (b) Hybrid printing of Mouse Embryonic Fibroblast (MEF) cells.

3. Results & Discussion

The presented algorithms are developed in Rhino3D software using Rhinoscript language. As mentioned before, Mimics software and its sample aorta MRI data is used to capture the initial geometry. The developed software is then used to generate cell and its support structures directly from the STL model of the aorta. The developed

algorithms finally outputs scripts which controls the cell and biomaterial heads to form the tissue constructs layer by layer.

NovoGel which is a bio-inert, thermo-responsive hydrogel was used for 3D printing of the ‘Cake’ and ‘Zigzag’ models. 2% (w/v) NovoGel was prepared with PBS with Ca2+ and Mg2+ salts. The solution was mixed with magnetic stirrer and it was micro waved for 1 minute on high power settings. Then, the solution was placed in a water bath set at 70°C. In order to obtain the sterilization conditions, NovoGel solution was sterilized using standard liquid sterilization procedures.

A uniformly flat surface is required for the printing process. Therefore, %2 Agarose solution was prepared with PBS and after sterilization process; 20 mL agarose solution is transferred into the petri dish bottom while ensuring it covers the entire dish surface. Using aseptic technique, the sterilized mold was slowly lowered onto the Agarose inside the petri dish. After the agarose solution was completely gel, the mold was carefully pulled away from the petri dish.

For demonstration purpose colored hydrogel is used to represent cells. In order to print the ‘Cake’ and ‘ZigZag’ models bicolored, NovoGel was stained with % 0.5 (w/v) Phenol Red solution which is suitable for cell culture. % 0.5 (w/v) Phenol Red solution is prepared with deionized water. During the preparation of the materials, adequate sterilization conditions are provided to prevent any contamination.

First, ‘cake’ model is printed as shown in Fig. 7. As shown in the figure, the dyed hydrogel (red) is used to represent cell cylinders. The cell-representing hydrogel filaments are successfully printed at the channels formed by the support material (hydrogel).

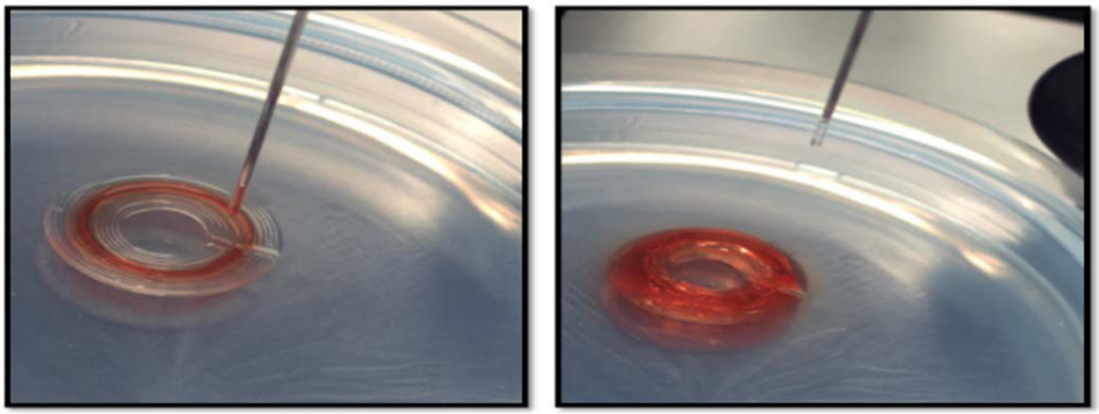

Fig. 7. 3D Printed stained hydrogel (representing cells) and its cake-like support structure (8 layers).

Unlike the ‘cake’ pattern, zigzag model can be used for more complex tissue constructs. The model shown in Fig. 4 is printed using ‘zig-zag’ pattern. Fig. 8 shows the printed bicolored hydrogels. Again, the red colored hydrogel represents cylindrical cell aggregates. As shown in the figure, the support structure didn’t form very well because of the nature of hydrogel. The viscoelastic nature of hydrogels makes the printed cylinders to be deformed. This could be further optimized by adjusting the design and 3D printing parameters.

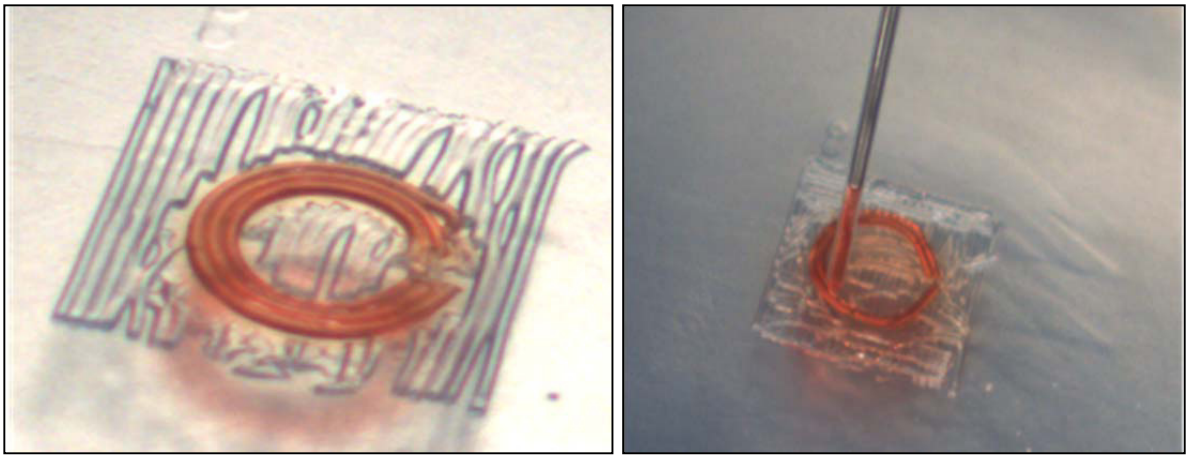

Fig. 8. 3D Printing of support layers with zig-zag pattern.

4. Conclusion

In this paper, a novel path planning and optimization for 3D hybrid cell and biomaterial printing of macro vascular structure is presented. A part of aorta was segmented using an imaging and segmentation software. The captured geometry of the aorta was then converted to CAD model. Computational algorithms were developed generate support structures of cylindrical cell aggregates. A cake-like support structures is used for the aorta model. The cylindrical cell and support rods are always printed in between the previous layers support structures. For more complex shapes, support structures with a zig-zag pattern is used. The support layers are formed by crossing vertical and horizontal support rods at successive layers. Both methodology implemented on a CAD software package, Rhino3D using rhinoscript language. The developed software generated instruction for the 3D bioprinter. Example cake and zig-zag pattern support structures printed layer by layer using a bicolored Novogel hydrogel.

Acknowlegments

This research is supported by The Scientific and Technological Research Council of Turkey (TUBITAK) grant number 112M094 and the Sabanci University.

References

[1] Nemeno-Guanzon J. G., Lee S., Berg J. H., Jo Y. H., Yeo J. E., Nam B. M., Koh Y., Lee J. I., Trends in tissue engineering for blood vessels, Journal of Biomedicine and Biotechnology, (2012).

[2] Novosel E. C., Kleinhans C., Kluger P. J., Vascularization is the key challenge in tissue engineering, Advanced Drug Delivery Reviews, 63, 300-311, (2011).

[3] Jakab K., Norotte C., Marga F., Murphy K., Vunjak-Novakovic G., Forgacs G., Tissue engineering by self-assembly and bioprinting of living cells, Biofabrication, 2:022001 (2010).

[4] Norotte C., Marga F. S., Niklason L. E., Forgacs G., Scaffold-free vascular tissue engineering using bioprinting, Biomaterials, 30, 5910–7, (2009).

[5] Marga F., Jakab K., Khatiwala C., Shepherd B., Dorfman S., Hubbard B., Colbert S., Gabor F., Toward engineering functional organ modules by additive manufacturing, Biofabrication, 4: 022001, (2012).

[6] Faulkner-Jones A., Greenhough S., King J. A., Gardner J., Courtney A., Shu W., Development of a valve-based cell printer for the formation of human embryonic stem cell spheroid aggregates, Biofabrication, 5:015013, (2013).

[7] Domingos, M., et al., Evaluation of in vitro degradation of PCL scaffolds fabricated via BioExtrusion – Part 2: Influence of pore size and geometry. Virtual and Physical Prototyping, 2011. 6(3): p. 157-165.

[8] Khoda, A., I.T. Ozbolat, and B. Koc, A functionally gradient variational porosity architecture for hollowed scaffolds fabrication. Biofabrication, 2011. 3(3): p. 1-15.
[9] Khoda, A.K.M.B., I.T. Ozbolat, and B. Koc, Engineered Tissue Scaffolds With Variational Porous Architecture. Journal of Biomechanical Engineering, 2011. 133(1): p. 011001.
[10] Melchels, F.P.W., et al., Effects of the architecture of tissue engineering scaffolds on cell seeding and culturing. Acta Biomaterialia, 2010. 6(11): p. 4208-4217.
[11] Khoda, A.B., I.T. Ozbolat, and B. Koc, Designing Heterogeneous Porous Tissue Scaffolds for Additive Manufacturing Processes. Journal of Computer Aided Design (CAD) (Accepted with minor revision CAD-D-12-00309), 2013.
[12] Gaetani, R., et al., Cardiac tissue engineering using tissue printing technology and human cardiac progenitor cells. Biomaterials, 2012. 33(6): p. 1782-1790.